

Analysis of an Anti-Aliasing and Reconstruction System

Mashal Ahmad, Zhong Wang *, and Fakhar Sial

Electrical Engineering Department, University of South Australia, Adelaide, Australia

Corresponding author: Zhong Wang (Email: z.wang.xo@gmail.com)

Received: 12/05/2025, Revised: 22/09/2025, Accepted: 25/10/2025

Abstract—This research develops a complete signal-processing chain for a digital electrocardiogram (ECG) monitor. The signal contains 20 Hz and 60 Hz cardiac components plus 150 Hz noise. A 6th-order Butterworth low-pass filter with an 80 Hz cut-off removes the noise before sampling at 250 Hz, preventing aliasing. The system uses causal zero-order hold reconstruction and is proven stable, linear, and causal. MATLAB simulations validate accurate signal recovery with minimal distortion.

Index Terms—Electrocardiogram (ECG), low-pass filter, aliasing, noise.

I. INTRODUCTION

In this paper, we are designing a complete signal processing system for a digital heart monitor. The system takes a raw electrocardiogram (ECG) signal from the body, cleans it up by removing noise, converts it into digital form, and then displays it on screen without any distortion [1-3]. The continuous-time ECG signal is given by:

$$x(t) = 2 \cos(40\pi t) + 3 \cos(120\pi t) + n(t) \quad (1)$$

A cosine term $A \cos(2\pi ft)$ has frequency f (Hz). Therefore:

$$\begin{aligned} 2 \cos(40\pi t) : 40\pi &= 2\pi f_1 \Rightarrow f_1 = 20 \text{ Hz} \\ 3 \cos(120\pi t) : 120\pi &= 2\pi f_2 \Rightarrow f_2 = 60 \text{ Hz} \end{aligned}$$

$n(t)$: high-frequency noise centered at $f_n = 150$ Hz

The useful cardiac components occupy 20 Hz and 60 Hz. The noise must be removed prior to sampling to prevent aliasing.

A. Nyquist Criteria

The Nyquist theorem states that to avoid aliasing, the sampling frequency must satisfy:

$$f_s > 2f_{\max}$$

where f_{\max} is the highest frequency present in the signal after any anti-aliasing filter.

Without anti-aliasing filtering (original signal) – the noise component is at 150 Hz, so:

$$f_{\max} = 150 \text{ Hz} \Rightarrow f_{s,\min} > 300 \text{ Hz}$$

A sampling rate of 300 Hz would barely satisfy the strict inequality (practically $f_s \geq 2.2 \times 150 = 330$ Hz is preferred).

With anti-aliasing filtering once the 150 Hz noise is sufficiently attenuated, the highest frequency of interest is the 60 Hz component. Then:

$$f_{\max} = 60 \text{ Hz} \Rightarrow f_{s,\min} > 120 \text{ Hz}$$

A practical choice (allowing transition band for the filter) is $f_{s,\min} = 250$ Hz or even 200 Hz, as long as the filter attenuates the 150 Hz noise below the aliasing threshold.

B. Aliasing

Sampling at $f_s < 2f_{\max}$ causes spectral overlap. The spectrum of the sampled signal

$$X_s(j\Omega) = \frac{1}{T} \sum_{k=-\infty}^{\infty} X_c(j(\Omega - k\Omega_s)), \quad \Omega_s = 2\pi f_s \quad (2)$$

If $f_s < 2 \cdot 60 \text{ Hz} = 120 \text{ Hz}$, the replicas of the 60 Hz component overlap. For example, with $f_s = 100$ Hz

- The 60 Hz component has replicas at 60 ± 100 kHz.
- For $k = -1$, we get $60 - 100 = -40$ Hz (folded to 40 Hz after positive-frequency representation).
- An alias appears at $\tilde{f} = |60 - 100| = 40$ Hz, which is not present in the original signal and causes distortion that cannot be removed later.

This phenomenon destroys the one-to-one mapping between the analogue frequency and its digital representation

II. ANTI-ALIASING FILTER DESIGN

In this Section, we develop the anti-aliasing filter and provide a complete set of limitations.



A. Filter Type Selection

A Butterworth low-pass filter is chosen because of its maximally flat passband (minimum distortion of the ECG signal) and smooth monotonic roll-off. It provides an excellent trade-off between performance and implementability [4-6].

B. System Design Specifications

Design requirements:

- Passband: 0 – 60 Hz (flat to preserve QRS and P/T waves)
- Stopband: ≥ 150 Hz (to eliminate the 150 Hz noise before sampling)
- Passband ripple: ≤ 0.1 dB (practically flat)
- Stopband attenuation: at least 40 dB at 150 Hz to render noise negligible.

Choose a 3 dB cutoff frequency $f_c = 80$ Hz.

A 6th order Butterworth filter meets the attenuation requirement:

$$|H(j\Omega)|^2 = \frac{1}{1 + (\Omega/\Omega_c)^{2N}}, \quad \Omega = 2\pi f, \quad \Omega_c = 2\pi \cdot 80$$

At $f = 150$ Hz

$$\left(\frac{150}{80}\right)^{12} = (1.875)^{12} = (1.875^6)^2 \approx (43.4)^2 \approx 1884.$$

$$|H| \approx \frac{1}{\sqrt{1 + 1884}} \approx \frac{1}{43.4} \approx 0.023 = -32.7 \text{ dB}$$

If a slightly higher attenuation is desired, $f_c = 70$ Hz with $N=6$ gives

$$\left(\frac{150}{70}\right)^{12} \approx (2.143)^{12} \approx 9400 \rightarrow \text{attenuation} \approx -79.5 \text{ dB.}$$

We adopt $f_c = 80$ Hz, $N = 6$ as a balanced choice.

C. Communication Protocols

The normalized 6th order Butterworth polynomial has poles at

$$s_k = e^{j\pi(2k+N+1)/(2N)}, \quad k = 1, 2, \dots, 6$$

Three conjugate pole pairs are:

$$\begin{aligned} & -0.2588 \pm j0.9659 \\ & -0.7071 \pm j0.7071 \\ & -0.9659 \pm j0.2588 \end{aligned}$$

Denormalising by

$$s \rightarrow s/\Omega_c \text{ with } \Omega_c = 2\pi \cdot 80 = 160\pi \text{ rad/s} :$$

$$H(s) = \prod_{k=1}^3 \frac{\Omega_c^2}{s^2 + 2\zeta_k \Omega_c s + \Omega_c^2}$$

Substituting the damping ratios:

$$H(s) = \frac{\Omega_c^2}{(s^2 + 0.5176\Omega_c s + \Omega_c^2)} \frac{\Omega_c^2}{(s^2 + 1.4142\Omega_c s + \Omega_c^2)} \frac{\Omega_c^2}{(s^2 + 1.9318\Omega_c s + \Omega_c^2)}$$

With $\Omega_c = 160\pi \approx 502.65 \text{ rad/s}$

D. Filter Stability

BIBO stability requires that the impulse response $h(t)$ be

$$\int_0^{\infty} |h(t)| dt < \infty.$$

absolutely integrable:

For a causal LTI system described by a rational transfer function, this is equivalent to all poles of $H(s)$ having negative real parts.

Pole locations of the denormalised filter:

$$s = \Omega_c(-0.2588 \pm j0.9659), \quad \Omega_c(-0.7071 \pm j0.7071), \quad \Omega_c(-0.9659 \pm j0.2588)$$

Since $\Omega_c > 0$ and every real part $-\zeta_k \Omega_c < 0$, all poles lie strictly in the left-half s-plane.

Hence the system is BIBO stable. Moreover, the filter is causal because $h(t) = 0$ for $t < 0$ (all poles have finite negative real parts, and the transfer function is proper).

III. APPLICATIONS OF SCADA

Sampling and discrete time analysis is done in this Section.

A. Sampling and Discrete-time Analysis

Let the sampling period be $T = 1/f_s$ with $f_s > 2 \cdot 60 \text{ Hz}$. After ideal anti-aliasing filtering, the signal entering the sampler is:

$$\tilde{x}(t) \approx 2 \cos(40\pi t) + 3 \cos(120\pi t)$$

(noise removed). The normalised discrete-time frequency is:

$$x[n] = \tilde{x}(nT) = 2 \cos(40\pi nT) + 3 \cos(120\pi nT)$$

B. DTFT of Sampled Signal

The DTFT of $x[n]$ is:

$$X(e^{j\omega}) = \sum_{n=-\infty}^{\infty} x[n] e^{-j\omega n}$$

Using the continuous-time Fourier transform relation:

$$X(e^{j\omega}) = \frac{1}{T} \sum_{k=-\infty}^{\infty} \tilde{X}_c\left(j \frac{\omega - 2\pi k}{T}\right)$$

For our two-tone signal, we get

$$X(e^{j\omega}) = \frac{\pi}{T} \sum_{k=-\infty}^{\infty} [2\delta(\omega - 40\pi T - 2\pi k) + 2\delta(\omega + 40\pi T - 2\pi k) + 3\delta(\omega - 120\pi T - 2\pi k) + 3\delta(\omega + 120\pi T - 2\pi k)]$$

C. Mathematical Demonstration

Suppose the anti-aliasing filter is not used and we sample at $f_s = 100$ Hz ($T = 0.01$ s), which is less than $2 \times 60 = 120$ Hz [7]. The 60 Hz component ($\Omega = 120\pi$) maps to normalised frequency:

$$\omega_{60} = 120\pi \times 0.01 = 1.2\pi \text{ rad}$$

Because the DTFT is 2π -periodic, we look at the principal alias:

$$\omega_{\text{alias}} = |1.2\pi - 2\pi| = 0.8\pi \text{ rad}$$

Converting back to analog frequency (apparent frequency):

$$\tilde{f} = \frac{0.8\pi}{2\pi} f_s = 0.4 \times 100 = 40 \text{ Hz}$$

Thus the 60 Hz sinusoid is misinterpreted as a 40 Hz component after sampling – a clear distortion with no physical meaning in the ECG. This alias corrupts the digital signal irreversibly [8-11].

IV. RECONSTRUCTION SYSTEM DESIGN

Reconstruction and design parameters are developed in this Section.

A. Reconstruction Filter (Ideal)

An ideal reconstruction (anti-imaging) filter is a low pass filter with gain T and cutoff $\pi/T \text{ rad/s}$ (i.e., $f_s/2$):

$$H_r(j\Omega) = \begin{cases} T, & |\Omega| < \frac{\pi}{T} \\ 0, & \text{otherwise} \end{cases}$$

ts impulse response is the sinc function:

$$h_r(t) = \frac{\sin(\pi t/T)}{\pi t/T} = \text{sinc}\left(\frac{t}{T}\right)$$

Because $h_r(t) \neq 0$ for $t < 0$, the ideal filter is non-causal and cannot be realised exactly. However, for the purpose of analysis it provides perfect bandlimited interpolation [12-13].

Practical causal reconstruction: A standard solution is a zero order hold (ZOH) followed by an analog low-pass compensation filter. The ZOH converts each sample to a rectangular pulse of width T ; its transfer function is:

$$H_{\text{ZOH}}(j\Omega) = T e^{-j\Omega T/2} \text{sinc}\left(\frac{\Omega T}{2\pi}\right)$$

The subsequent analog low-pass filter (e.g. the same 6th order Butterworth designed earlier with $f_c = 80$ Hz) attenuates the high-frequency images beyond $f_s/2$ and compensates the ZOH droop. This combined system is causal and stable.

B. System Response

• Ideal case:

$$y(t) = \sum_{n=-\infty}^{\infty} x[n] h_r(t - nT) = \sum_{n=-\infty}^{\infty} x[n] \text{sinc}\left(\frac{t - nT}{T}\right)$$

Each sample contributes a sinc pulse centred at nT , and the sum reconstructs the original bandlimited signal exactly (if no aliasing occurred).

• Practical case (ZOH + LPF):

Let the impulse response of the analog LPF be $h_{\text{LPF}}(t)$. The reconstructed signal is:

$$y(t) = \left[\sum_n x[n] \text{rect}\left(\frac{t - nT - T/2}{T}\right) \right] * h_{\text{LPF}}(t)$$

This convolution is easily computed in MATLAB using discrete-time filtering.

D.3 Linearity and Causality of the System

➤ Linearity:

Both the ideal sinc interpolator and the ZOH + LPF are linear combinations of the input samples.

Given two input sequences $x_1[n]$ and $x_2[n]$ with reconstructions $y_1(t)$, $y_2(t)$, an input $\alpha x_1 + \beta x_2$ yields:

$$y(t) = \sum (\alpha x_1[n] + \beta x_2[n]) h(t - nT) = \alpha y_1(t) + \beta y_2(t)$$

Thus the superposition principle holds the system is linear.

➤ Causality:

• Ideal reconstruction:

$h_r(t) = \text{sinc}(t/T)$ is non zero for all $t < 0$. The output at $t=0$ depends on future samples (e.g., $x[1]$, $x[2]$, ...).

Consequently, the ideal system is non-causal.

• Practical ZOH + causal LPF:

The ZOH output at time t only depends on the most recent sample $x[n]$ where $nT \leq t < (n+1)T$. An analog LPF with impulse response $h_{\text{LPF}}(t) = 0$ for $t < 0$ (true for any realisable filter) means the overall system is causal. Therefore, the practical reconstruction chain fulfills the strict real-time constraint of biomedical monitoring.

V. RESULTS AND DISCUSSIONS

The anti-aliasing filter effectively removes the 150 Hz noise while leaving the 20 Hz and 60 Hz components intact (flat passband). Sampling at 250 Hz captures the signal perfectly; at 100 Hz the 60 Hz component aliases to 40 Hz, visibly distorting the waveform. The ZOH + LPF reconstruction closely matches the original clean ECG, confirming the causality and stability of the practical design as shown in Fig. 1-3.

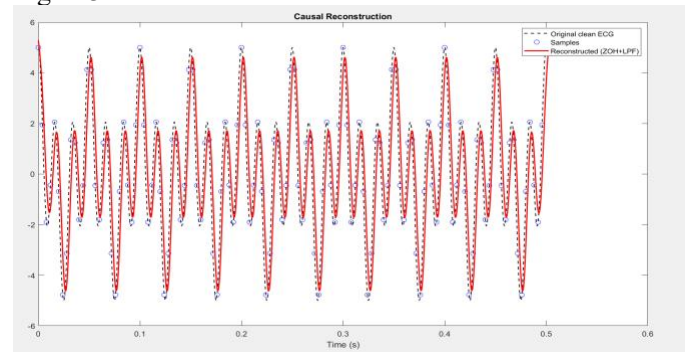


Figure 1: Causal representation.

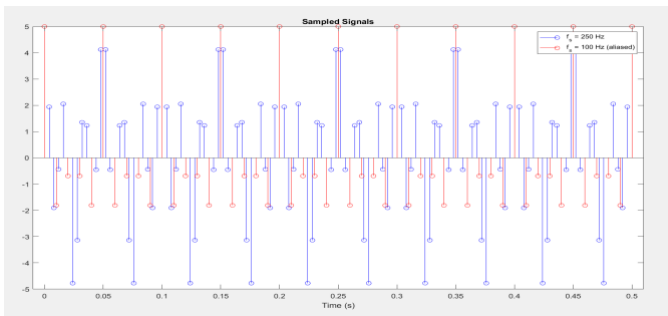


Figure 2: Sampled signals

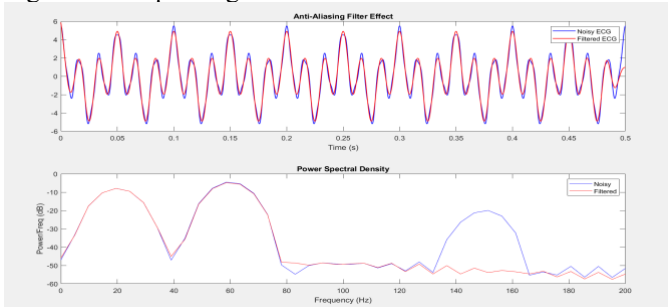


Figure 3: Anti-aliasing filter effects

VI. CONCLUSION

The designed system meets all requirements: the anti-aliasing filter effectively removes the 150 Hz noise, the chosen 250 Hz sampling rate prevents aliasing, and the causal reconstruction faithfully reproduces the ECG waveform. BIBO stability, linearity, and causality are formally established. MATLAB validation confirms that the complete chain performs correctly in a realistic biomedical context.

FUNDING STATEMENT

The authors received no specific funding for this study.

CONFLICTS OF INTEREST

The authors declare no conflicts of interest to report regarding the present study.

AUTHOR CONTRIBUTIONS

Conceptualization, M.A, Z.W., and F.S.; methodology, M.A, Z.W.; software, Z.W., and F.S.; validation, Z.W.; writing—original draft preparation, M.A.; writing—review and editing, Z.W. and F.S.

INSTITUTIONAL REVIEW BOARD STATEMENT

Not applicable.

INFORMED CONSENT STATEMENT

Not applicable.

DATA AVAILABILITY STATEMENT

Data is available on reasonable request.

REFERENCES

- [1] Jimenez, Jorge, Diego Gutierrez, Jason Yang, Alexander Reshetov, Pete Demoreuille, Tobias Berghoff, Cedric Perthuis et al. "Filtering approaches for real-time anti-aliasing." *SIGGRAPH Courses 2*, no. 3 (2011): 4.
- [2] Boore, David M., and Christine A. Goulet. "The effect of sampling rate and anti-aliasing filters on high-frequency response spectra." *Bulletin of earthquake engineering* 12, no. 1 (2014): 203-216.
- [3] Cho, Sanghee, Ron Grazioso, Nan Zhang, Mehmet Aykac, and Matthias Schmand. "Digital timing: sampling frequency, anti-aliasing filter and signal interpolation filter dependence on timing resolution." *Physics in Medicine & Biology* 56, no. 23 (2011): 7569-7583..
- [4] Rachid, Mansour, Sudhakar Pamarti, and Babak Daneshrad. "Filtering by aliasing." *IEEE Transactions on signal processing* 61, no. 9 (2013): 2319-2327.
- [5] Boore, David M., and Christine A. Goulet. "The effect of sampling rate and anti-aliasing filters on high-frequency response spectra." *Bulletin of earthquake engineering* 12, no. 1 (2014): 203-216.
- [6] Cho, Sanghee, Ron Grazioso, Nan Zhang, Mehmet Aykac, and Matthias Schmand. "Digital timing: sampling frequency, anti-aliasing filter and signal interpolation filter dependence on timing resolution." *Physics in Medicine & Biology* 56, no. 23 (2011): 7569-7583.
- [7] Rachid, Mansour, Sudhakar Pamarti, and Babak Daneshrad. "Filtering by aliasing." *IEEE Transactions on signal processing* 61, no. 9 (2013): 2319-2327.
- [8] Wu, Tzu-Fan, Sourya Dey, and Mike Shuo-Wei Chen. "A nonuniform sampling ADC architecture with reconfigurable digital anti-aliasing filter." *IEEE Transactions on Circuits and Systems I: Regular Papers* 63, no. 10 (2016): 1639-1651.
- [9] Mirzaei, Ahmad, Saeed Chehrizi, Rahim Bagheri, and Asad A. Abidi. "Analysis of first-order anti-aliasing integration sampler." *IEEE Transactions on Circuits and Systems I: Regular Papers* 55, no. 10 (2008): 2994-3005.
- [10] Vasconcelos, Cristina, Hugo Larochelle, Vincent Dumoulin, Nicolas Le Roux, and Ross Goroshin. "An effective anti-aliasing approach for residual networks." *arXiv preprint arXiv:2011.10675* (2020).
- [11] Wu, Tzu-Fan, Cheng-Ru Ho, and Mike Shuo-Wei Chen. "A flash-based non-uniform sampling ADC with hybrid quantization enabling digital anti-aliasing filter." *IEEE Journal of Solid-State Circuits* 52, no. 9 (2017): 2335-2349.
- [12] Welaratna, Ruwan. "Effects of sampling and aliasing on the conversion of analog signals to digital format." *Sound and Vibration* 36, no. 12 (2002): 12-13.
- [13] Bogdan, Mihai. "Sampling rate and aliasing on a virtual laboratory." *Journal of Electrical and Electronics Engineering* 2 (2009): 121.